International Journal of Innovative Technologies
WWW.IJITECH.ORG
ISSN 2321-8665
Vol.04,Issue.01,
January-2016,
Pages:0012-0017

Quality Assessment of Fused Images

P. VINOD KUMAR[1], M. V. NARASIMHA REDDY[2], P. PRASANNA MURALI KRISHNA[3]

[1]PG Scholar, Dr. Samuel George Institute of Technology, Markapur, AP, India, Email: vindupesala@gmail.com.
[2]Assistant Professor, Dr. Samuel George Institute of Technology, Markapur, AP, India, Email: Narasimha0042008@gmail.com.
[2]Associate Professor, Dr. Samuel George Institute of Technology, Markapur, AP, India, Email: pprasannamurali@gmail.com.

Abstract: A fast and effective image fusion method is proposed for creating a highly informative fused image through merging multiple images. The proposed method is based on a two-scale decomposition of an image into a base layer containing large scale variations in intensity, and a detail layer capturing small scale details. A novel guided filtering-based weighted average technique is proposed to make full use of spatial consistency for fusion of the base and detail layers. Experimental results demonstrate that the proposed method can obtain state-of-the-art performance for fusion of multispectral, multifocus, multimodal, and multi-exposure images.

Keywords: Guided Filter, Spatial Consistency, Two-Scale Decomposition, Image Fusion.

I. INTRODUCTION

Image fusion is an important technique for various image processing and computer vision applications such as feature extraction and target recognition. Through image fusion, different images of the same scene can be combined into a single fused image [1]. The fused image can provide more comprehensive information about the scene which is more useful for human and machine perception. For instance, the performance of feature extraction algorithms can be improved by fusing multi-spectral remote sensing images [2]. The fusion of multi-exposure images can be used for digital photography [3]. In these applications, a good image fusion method has the following properties. First, it can preserve most of the useful information of different images. Second, it does not produce artifacts. Third, it is robust to imperfect conditions such as mis-registration and noise.A large number of image fusion methods [4]–[7] have been proposed in literature. Among these methods, multiscale image fusion [5] and data-driven image fusion [6] are very successful methods. They focus on different data representations, e.g., multi-scale coefficients [8], [9], or data driven decomposition coefficients [6], [10] and different image fusion rules to guide the fusion of coefficients. The major advantage of these methods is that they can well preserve the details of different source images. However, these kinds of methods may produce brightness and color distortions since spatial consistency is not well considered in the fusion process.

To make full use of spatial context, optimization based image fusion approaches, e.g., generalized random walks [3], and Markov random fields [11] based methods have been proposed. These methods focus on estimating spatially smooth and edgealigned weights by solving an energy function and then fusing the source images by weighted average of pixel values. However, optimization based methods have a common limitation, i.e., inefficiency, since they require multiple iterations to find the global optimal solution. Moreover, another drawback is that global optimization based methods may over-smooth the resulting weights, which is not good for fusion. To solve the problems mentioned above, a novel image fusion method with guided filtering is proposed in this paper. Experimental results show that the proposed method gives a performance comparable with state-of-the-art fusion approaches. Several advantages of the proposed image fusion approach are highlighted in the following.

- Traditional multi-scale image fusion methods require more than two scales to obtain satisfactory fusion results. The key contribution of this paper is to present a fast two-scale fusion method which does not rely heavily on a specific image decomposition method. A simple average filter is qualified for the proposed fusion framework.
- A novel weight construction method is proposed to combine pixel saliency and spatial context for image fusion. Instead of using optimization based methods, guided filtering is adopted as a local filtering method for image fusion.
- An important observation of this paper is that the roles of two measures, i.e., pixel saliency and spatial consistency are quite different when fusing different layers. In this paper, the roles of pixel saliency and spatial consistency are controlled through adjusting the parameters of the guided filter.

II. GUIDED IMAGE FILTERING

Recently, edge-preserving filters [12], [13] have been an active research topic in image processing. Edge-preserving smoothing filters such as guided filter [12], weighted least squares [13], and bilateral filter [14] can avoid ringing artifacts since they will not blur strong edges in the decomposition process. Among them, the guided filter is a

recently proposed edge-preserving filter, and the computing time of which is independent of the filter size. Furthermore, the guided filter is based on a local linear model, making it qualified for other applications such as image matting, up-sampling and colorization [12]. In this paper, the guided filter is first applied for image fusion.

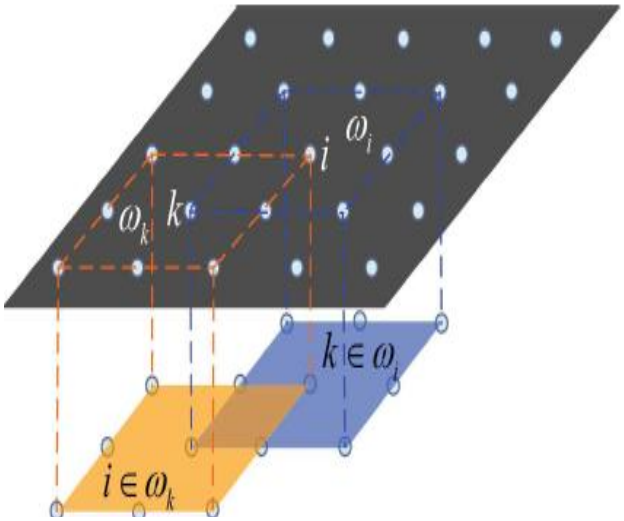

Fig.1. Illustration of window choice.

In theory, the guided filter assumes that the filtering output O is a linear transformation of the guidance image I in a local window ω_k centered at pixel k.

$$O_i = a_k I_i + b_k \ \forall i \in \omega_k \tag{1}$$

where ωk is a square window of size (2r+1)×(2r+1). The linear coefficients ak and bk are constant in ωk and can be estimated by minimizing the squared difference between the output image O and the input image P.

$$E(a_k, b_k) = \sum_{i \in \omega_k} \left((a_k I_i + b_k - P_i)^2 + \epsilon a_k^2 \right) \tag{2}$$

where ϵ is a regularization parameter given by the user.

The coefficients a_k and b_k can be directly solved by linear regression [15] as follows:

$$a_k = \frac{\frac{1}{|\omega|}\sum_{i \in \omega_k} I_i P_i - \mu_k \overline{P}_k}{\delta_k + \epsilon} \tag{3}$$

$$b_k = \overline{P}_k - a_k \mu_k \tag{4}$$

where μ_k and δ_k are the mean and variance of I in ω_k respectively, $|\omega|$ is the number of pixels in ω_k, and P_k is the mean of P in ω_k.

Next, the output image can be calculated according to (1). As shown in Fig. 1, all local windows centered at pixel k in the window ω_i will contain pixel i. So, the value of Oi in (1) will change when it is computed in different windows ω_k. To solve this problem, all the possible values of coefficients a_k and b_k are first averaged. Then, the filtering output is estimated as follows:

$$O_i = \overline{a}_i I_i + \overline{b}_i \tag{5}$$

Where $\overline{a}_i = \frac{1}{|\omega|}\sum_{k \in \omega_i} a_k$, $\overline{b}_i = \frac{1}{|\omega|}\sum_{k \in \omega_i} b_k$.

In this paper, $G_{r,\epsilon}(P, I)$ is used to represent the guided filtering operation, where r and ϵ are the parameters which decide the filter size and blur degree of the guided filter, respectively. Moreover, P and I refer to the input image and guidance image, respectively. Furthermore, when the input is a color image, the filtering output can be obtained by conducting the guided filtering on the red, green, and blue channels of the input image, respectively. And when the guidance image I is a color image, the guided filter should be extended by the following steps.

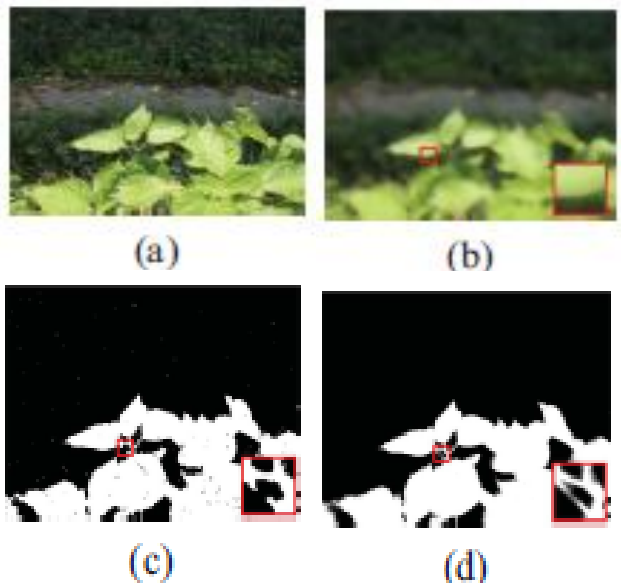

Fig. 2. Two examples of guided filtering. (a) and (c) are two input images of the guided filter. Image (b) is the filtered image (r=15, ϵ =0.3), with image (a) serving as the input image and the guidance image simultaneously. Image (d) is the filtered image (r = 10, ϵ = 10^{-6}), with images (a) and (c) serving as the guidance image and the input image, respectively.

First, equation (1) is rewritten as follows:

$$O_i = \mathbf{a}_k^T \mathbf{I}_i + b_k \ \forall i \in \omega_k \tag{6}$$

where $\mathbf{a}_k$ is a 3 × 1 coefficient vector and $\mathbf{I}i$ is a 3 × 1 color vector. Then, similar to (3)–(5), the output of guided filtering can be calculated as follows:

$$\mathbf{a}_k = (\Sigma_k + \epsilon U)\left(\frac{1}{|\omega|} \sum_{i \in \omega_k} \mathbf{I}_i p_i - \mu_k \overline{p}_k \right) \tag{7}$$

$$b_k = \overline{p}_k - \mathbf{a}_k^T \boldsymbol{\mu}_k \tag{8}$$

$$O_i = \overline{\mathbf{a}}_i^T \mathbf{I}_i + \overline{b}_i \tag{9}$$

Where Σ_k is the 3×3 covariance matrix of **I** in ωk, and U is the 3 × 3 identity matrix. For instance, Fig. 2(a) shows a color image of size 620×464. Guided filtering is conducted on each color channel of this image to obtain the color

filtered image shown in Fig. 2(b) (for this example, Fig. 2(a) serves as the guidance image and the input image simultaneously). As shown in the close-up view in Fig. 2(b), the guided filter can blur the image details while preserving the strong edges of the image. Fig. 2(c) and (d) give another example of guided filtering when the input image and guidance image are different. In this example, Fig. 2(c) and (a) serve as the input image and the color guidance image, respectively. It can be seen that the input image shown in Fig. 2(c) is noisy and not aligned with object boundaries. As shown in Fig. 2(d), after guided filtering, noisy pixels are removed and the edges in the filtered image are aligned with object boundaries. It demonstrates that those pixels with similar colors in the guidance image tend to have similar values in the filtering process.

III. IMAGE FUSION WITH GUIDED FILTERING

Fig3 summarizes the main processes of the proposed guided filtering based fusion method (GFF). First, an average filter is utilized to get the two-scale representations. Then, the base and detail layers are fused through using a guided filtering based weighted average method.

A. Two-Scale Image Decomposition

As shown in Fig3, the source images are first decomposed into two-scale representations by average filtering. The base layer of each source image is obtained as follows:

$$B_n = I_n * Z \tag{10}$$

where I_n is the nth source image, Z is the average filter, and the size of the average filter is conventionally set to 31×31.

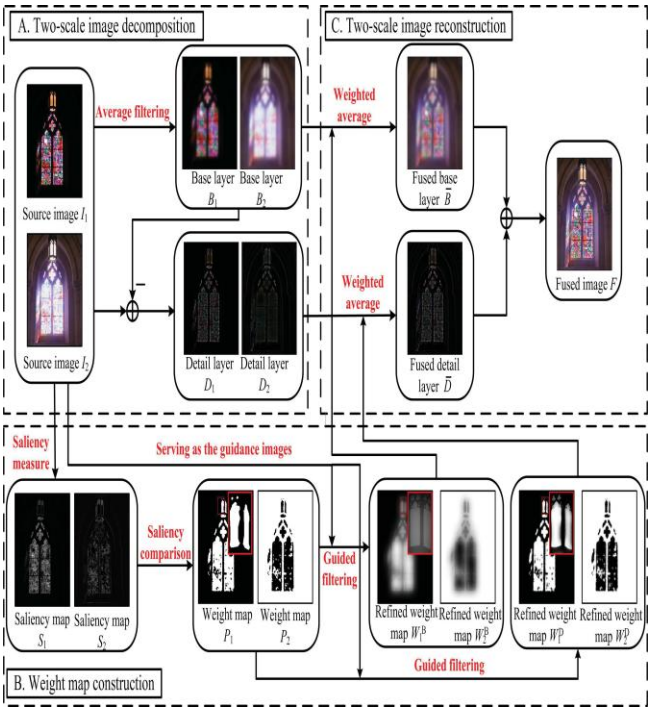

Fig.3. Schematic diagram of the proposed image fusion method based on guided filtering.

Once the base layer is obtained, the detail layer can be easily obtained by subtracting the base layer from the source image.

$$D_n = I_n - B_n. \tag{11}$$

The two-scale decomposition step aims at separating each source image into a base layer containing the large-scale variations in intensity and a detail layer containing the small scale details.

B. Weight Map Construction with Guided Filtering

As shown in Fig3, the weight map is constructed as follows. First, Laplacian filtering is applied to each source image to obtain the high-pass image

$$H_n = I_n * L \tag{12}$$

where L is a 3 × 3 Laplacian filter. Then, the local average of the absolute value of H_n is used to construct the saliency maps S_n.

$$S_n = |H_n| * g_{r_g,\sigma_g} \tag{13}$$

where g is a Gaussian low-pass filter of size $(2r_g + 1)$ $(2 r_g + 1)$, and the parameters r_g and $\sigma_g$are set to 5. The measured saliency maps provide good characterization of the saliency level of detail information. Next, the saliency maps are compared to determine the weight maps as follows:

$$P_n^k = \begin{cases} 1 \text{ if } S_n^k = \max\left(S_1^k, S_2^k, \ldots, S_N^k\right) \\ 0 \text{ otherwise} \end{cases} \tag{14}$$

where N is number of source images, S_n^k is the saliency value of the pixel k in the nth image. However, the weight maps obtained above are usually noisy and not aligned with object boundaries (see Fig. 3), which may produce artifacts to the fused image. Using spatial consistency is an effective way to solve this problem. Spatial consistency means that if two adjacent pixels have similar brightness or color, they will tend to have similar weights. A popular spatial consistency based fusion approach is formulating an energy function, where the pixel saliencies are encoded in the function and edge aligned weights are enforced by regularization terms, e.g., a smoothness term. This energy function can be then minimized globally to obtain the desired weight maps. However, the optimization based methods are often relatively inefficient. In this paper, an interesting alternative to optimization based methods is proposed. Guided image filtering is performed on each weight map P_n with the corresponding source image I_n serving as the guidance image

$$W_n^B = G_{r_1,\epsilon_1}(P_n, I_n) \tag{15}$$

$$W_n^D = G_{r_2,\epsilon_2}(P_n, I_n) \tag{16}$$

where r_1, ϵ_1, r_2, and ϵ_2 are the parameters of the guided filter, W_n^B and W_n^D are the resulting weight maps of the base and detail layers. Finally, the values of the N weight maps are normalized such that they sum to one at each pixel k. The motivation of the proposed weight construction method is as follows. According to (1), (3) and (4), it can be seen that if the local variance at a position i is very small which means that the pixel is in a flat area of the guidance image, then a_k will become close to 0 and the filtering output O will equal

to P_k, i.e., the average of adjacent input pixels. In contrast, if the local variance of pixel i is very large which means that the pixel i is in an edge area, then ak will become far from zero. As demonstrated in [12], $\nabla O \approx a\nabla I$ will become true, which means that only the weights in one side of the edge will be averaged. In both situations, those pixels with similar color or brightness tend to have similar weights. This is exactly the principle of spatial consistency.

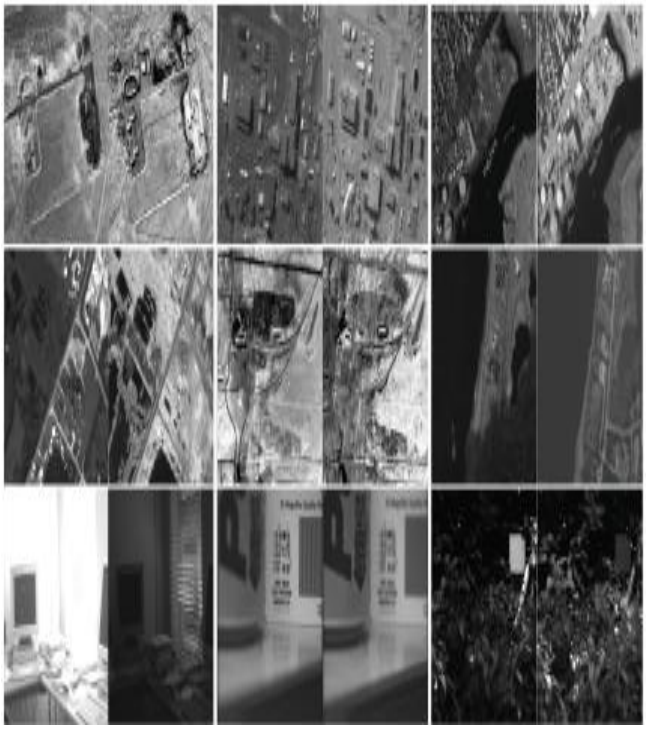

Fig. 4. Illustrations of nine pairs of testing images of the Petrovi´c database.

Furthermore, as shown in Fig3, the base layers look spatially smooth and thus the corresponding weights also should be spatially smooth. Otherwise, artificial edges may be produced. In contrast, sharp and edge-aligned weights are preferred for fusing the detail layers since details may be lost when the weights are over-smoothed. Therefore, a large filter size and a large blur degree are preferred for fusing the base layers, while a small filter size and a samll blur degree are preferred for the detail layers.

C. Two-Scale Image Reconstruction

Two-scale image reconstruction consists of the following two steps. First, the base and detail layers of different source images are fused together by weighted averaging

$$\overline{B} = \sum_{n=1}^{N} W_n^B B_n \tag{17}$$

$$\overline{D} = \sum_{n=1}^{N} W_n^D D_n \tag{18}$$

Then, the fused image F is obtained by combining the fused base layer $\overline{B}$ and the fused detail layer $\overline{D}$

$$F = \overline{B} + \overline{D}. \tag{19}$$

IV. RESULTS AND DISCUSSION

(a)

(b)

Fig5. Input images (a) & (b) for fusion.

Fig6. Fused image of curvelet

Fig6. Fused image of DCT.

Fig7. Fused image of MSWT.

Fig8. Fused image of SWT.

Fig9. Fused image of GF

Table1. Quality matrices of fused image (a) & (b)

Quality matrices	Curvolet transform	Stationary wavelet trans	Multi stationary wave	Discrete wavelets	Guided filter
Mean	1.1367e+005	1.1337e+005	1.1337e+004	1.1337e+005	1.1334e+005
Standard deviation	2.3724e+004	2.1681e+004	2.1748e+04	2.2000e+04	2.3959e+04
Entropy	4.7023	4.6290	4.5220	4.8731	4.5838
SSIM	0.987	0.9684	0.9638	0.9517	0.9976

V. CONCLUSION

We have presented a novel image fusion method based on guided filtering. The proposed method utilizes the average filter to get the two-scale representations, which is simple and effective. More importantly, the guided filter is used in a novel way to make full use of the strong correlations between neighborhood pixels for weight optimization . Experiments show that the proposed method can well preserve the original and complementary information of multiple input images. Encouragingly, the proposed method is very robust to image registration. Furthermore, the proposed method is computationally efficient, making it quite qualified for real applications. At last, how to improve the performance of the proposed method by adaptively choosing the parameters of the guided filter can be further researched.

VI. REFERENCES

[1] A. A. Goshtasby and S. Nikolov, “Image fusion: Advances in the state of the art,” Inf. Fusion, vol. 8, no. 2, pp. 114–118, Apr. 2007.

[2] D. Socolinsky and L. Wolff, “Multispectral image visualization through first-order fusion,” IEEE Trans. Image Process., vol. 11, no. 8, pp. 923–931, Aug. 2002.

[3] R. Shen, I. Cheng, J. Shi, and A. Basu, "Generalized random walks for fusion of multi-exposure images," IEEE Trans. Image Process., vol. 20, no. 12, pp. 3634–3646, Dec. 2011.
[4] S. Li, J. Kwok, I. Tsang, and Y. Wang, "Fusing images with different focuses using support vector machines," IEEE Trans. Neural Netw., vol. 15, no. 6, pp. 1555–1561, Nov. 2004.
[5] G. Pajares and J. M. de la Cruz, "A wavelet-based image fusion tutorial," Pattern Recognit., vol. 37, no. 9, pp. 1855–1872, Sep. 2004.
[6] D. Looney and D. Mandic, "Multiscale image fusion using complex extensions of EMD," IEEE Trans. Signal Process., vol. 57, no. 4, pp. 1626–1630, Apr. 2009.
[7] M. Kumar and S. Dass, "A total variation-based algorithm for pixellevel image fusion," IEEE Trans. Image Process., vol. 18, no. 9, pp. 2137–2143, Sep. 2009.
[8] P. Burt and E. Adelson, "The laplacian pyramid as a compact image code," IEEE Trans. Commun., vol. 31, no. 4, pp. 532–540, Apr. 1983.
[9] O. Rockinger, "Image sequence fusion using a shift-invariant wavelet transform," in Proc. Int. Conf. Image Process., vol. 3, Washington, DC, USA, Oct. 1997, pp. 288–291.
[10] J. Liang, Y. He, D. Liu, and X. Zeng, "Image fusion using higher order singular value decomposition," IEEE Trans. Image Process., vol. 21, no. 5, pp. 2898–2909, May 2012.
[11] M. Xu, H. Chen, and P. Varshney, "An image fusion approach based on markov random fields," IEEE Trans. Geosci. Remote Sns., vol. 49, no. 12, pp. 5116–5127, Dec. 2011.
[12] K. He, J. Sun, and X. Tang, "Guided image filtering," in Proc. Eur. Conf. Comput. Vis., Heraklion, Greece, Sep. 2010, pp. 1–14.
[13] Z. Farbman, R. Fattal, D. Lischinski, and R. Szeliski, "Edge-preserving decompositions for multi-scale tone and detail manipulation," ACM Trans. Graph., vol. 27, no. 3, pp. 67-1–67-10, Aug. 2008.
[14] F. Durand and J. Dorsey, "Fast bilateral filtering for the display of highdynamic- range images," ACM Trans. Graph., vol. 21, no. 3, pp. 257–266, Jul. 2002.
[15] N. Draper and H. Smith, Applied Regression Analysis. New York, USA: Wiley, 1981.
[16] V. Petrovi´c, "Subjective tests for image fusion evaluation and objective metric validation," Inf. Fusion, vol. 8, no. 2, pp. 208–216, Apr. 2007.
[17] G. Piella, "Image fusion for enhanced visualization: A variational approach," Int. J. Comput. Vision, vol. 83, pp. 1–11, Jun. 2009.
[18] S. Li, X. Kang, J. Hu, and B. Yang, "Image matting for fusion of multi-focus images in dynamic scenes," Inf. Fusion, vol. 14, no. 2, pp. 147–162, 2013.
[19] L. Tessens, A. Ledda, A. Pizurica, and W. Philips, "Extending the depth of field in microscopy through curvelet-based frequency-adaptive image fusion," in Proc. IEEE Int. Conf. Acoust. Speech Signal Process., vol. 1, Apr. 2007, pp. 861–864.
[20] Q. Zhang and B. Guo, "Multifocus image fusion using the nonsubsampled contourlet transform," Signal Process., vol. 89, no. 7, pp. 1334–1346, Jul. 2009.
[21] J. Tian and L. Chen, "Adaptive multi-focus image fusion using a waveletbased statistical sharpness measure," Signal Process., vol. 92, no. 9, pp. 2137–2146, Sep. 2012.
[22] M. Hossny, S. Nahavandi, and D. Creighton, "Comments on 'information measure for performance of image fusion'," Electron. Lett., vol. 44, no. 18, pp. 1066–1067, Aug. 2008.
[23] C. Yang, J. Zhang, X. Wang, and X. Liu, "A novel similarity based quality metric for image fusion," Inf. Fusion, vol. 9, no. 2, pp. 156–160,Apr. 2008.
[24] N. Cvejic, A. Loza, D. Bull, and N. Canagarajah, "A similarity metric for assessment of image fusion algorithms," Int. J. Signal Process., vol. 2,no. 3, pp. 178–182, Apr. 2005.
[25] C. Xydeas and V. Petrovi´c, "Objective image fusion performance measure," Electron. Lett., vol. 36, no. 4, pp. 308–309, Feb. 2000.
[26] J. Zhao, R. Laganiere, and Z. Liu, "Performance assessment of combinative pixel-level image fusion based on an absolute feature measurement," Int. J. Innovative Comput. Inf. Control, vol. 3, no. 6, pp. 1433–1447, Dec. 2007.
[27] Z. Liu, E. Blasch, Z. Xue, J. Zhao, R. Laganiere, and W. Wu, "Objective assessment of multiresolution image fusion algorithms for context enhancement in night vision: A comparative study," IEEE Trans. Pattern Anal. Mach. Intell., vol. 34, no. 1, pp. 94–109, Jan. 2012.
[28] G. Qu, D. Zhang, and P. Yan, "Information measure for performance of image fusion," Electron. Lett., vol. 38, no. 7, pp. 313–315, Mar. 2002.
[29] Z. Wang, A. Bovik, H. Sheikh, and E. Simoncelli, "Image quality assessment: From error visibility to structural similarity," IEEE Trans. Image Process., vol. 13, no. 4, pp. 600–612, Apr. 2004.
[30] Z. Wang and A. Bovik, "A universal image quality index," IEEE Signal Process. Letters, vol. 9, no. 3, pp. 81–84, Mar. 2002.
[31] F. C. Crow, "Summed-area tables for texture mapping," in Proc. SIGGRAPH 84. 11th Annu. Conf. Comput. Graph. Interact. Tech., vol. 18, no. 3, pp. 207–212, Jan. 1984.